

Supporting Information

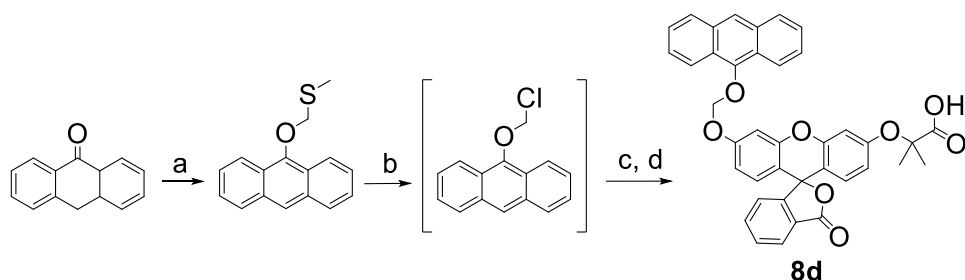
Hybrids of a 9-anthracenyl moiety and fluorescein as chemodosimeters for detection of singlet oxygen in live cells

Serghei Chercheja, Steffen Daum, Honggui Xu, Frank Beierlein, and Andriy Mokhir*

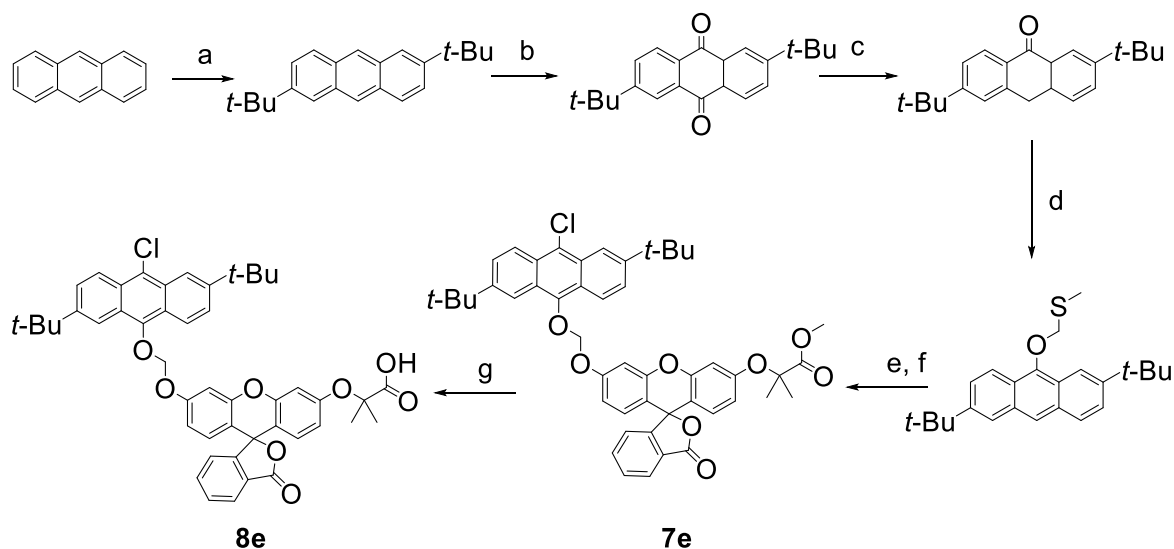
Content

Outline of synthesis of probes 8d and 8e	p. S2
NMR spectra of intermediates and new singlet oxygen probes	p. S3-S14
Calculation of energies of highest occupied orbitals (HOMOs) of simple models mimicking probes 4 , 8a-e	p. S15-S16
¹ H NMR spectroscopic monitoring of the reaction of probe 4 with ¹ O ₂ .	p. S17
Detection of ¹ O ₂ in prostate cancer cells DU-145 monitored by using fluorescence microscopy in combination with probe 4 .	p. S18
References	p. S19

Outline of synthesis of probes **8d** and **8e**



Scheme S1. Synthesis of probe **8d**: a) chloromethyl methyl sulfide, NaH, DMSO, rt, 24 h, 7%; (b) SO₂Cl₂, CH₂Cl₂, 22 °C, 1 h; (c) compound **6**, *t*-BuOK, DMF, rt, 24 h; d) LiOH, H₂O/THF, 22 °C, 24 h, (2% over 2 steps).



Scheme S2. Synthesis of probe **8e**: (a) according to (1). Whitton, A. J.; Kumberger, O.; Müller, G.; Schmidbaur, H. *Chem. Ber.* **1990**, *123*, 1931-1939 and (2) Whitton, A. J.; Kumberger, O.; Müller, G.; Schmidbaur, H. *Chem. Ber.* **1990**, *123*, 1931-1939: *t*-BuCl, AlCl₃, CHCl₃, reflux, 24 h, 34%; (b) according to U. Müller, V. Enkelmann, M. Adam and K. Müllen, *Chemische Berichte* **1993**, *126*, 1217-1225: (NH₄)₂Ce(NO₃)₆, THF/H₂O, rt, 2 h, 64%; (c) according to Müller, U.; Enkelmann, V.; Adam, M.; Müllen, K. *Chem. Ber.* **1993**, *126*, 1217-1225 and Müller, U.; Enkelmann, V.; Adam, M.; Müllen, K. *Chem. Ber.* **1993**, *126*, 1217-1225: Sn, AcOH, HCl, 81%; (d) Chloromethyl methyl sulfide, NaH, DMSO, rt, 18 h, 5%; (e) SO₂Cl₂, CH₂Cl₂, rt, 1 h; (f) compound **6**, *t*-BuOK, DMF, rt, 24 h, 11%; (g) LiOH, H₂O/THF, rt, 24 h, 15%.

NMR spectra of intermediates and new singlet oxygen probes 4, 8b-8e

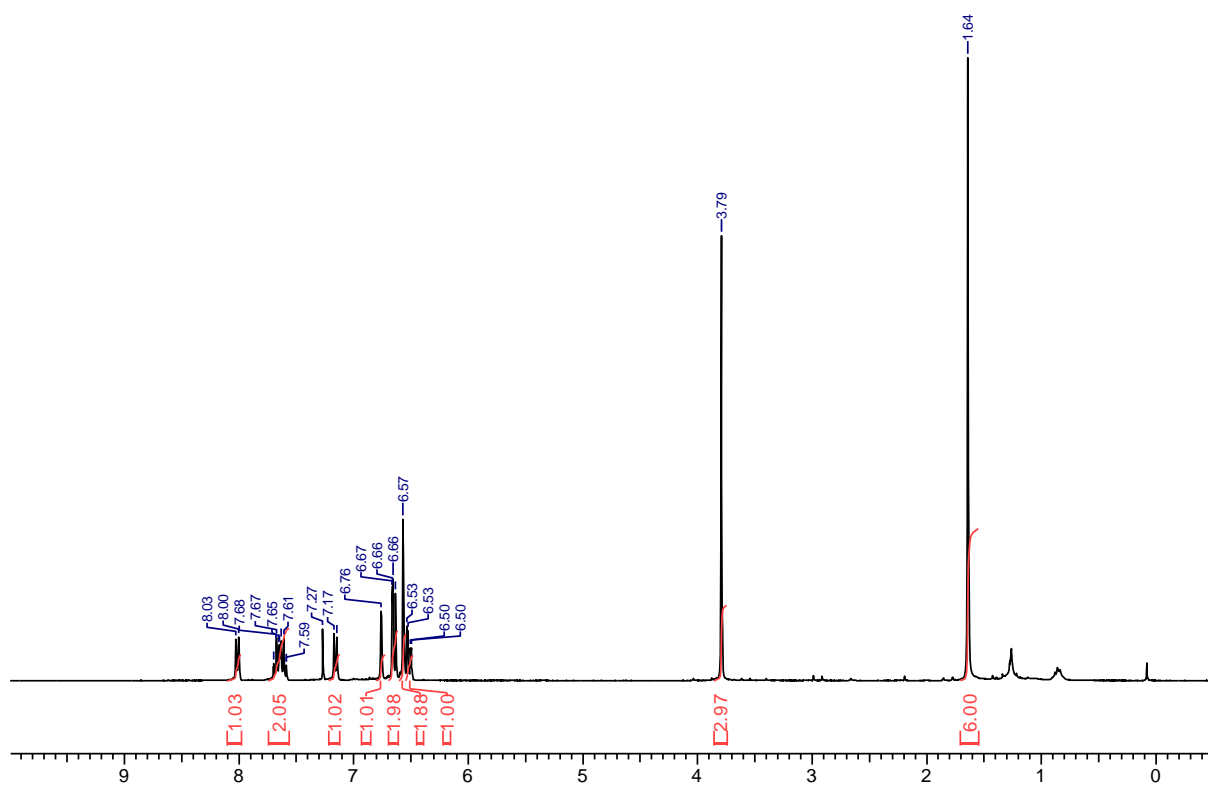


Figure S1. ^1H NMR spectrum of compound **6**.

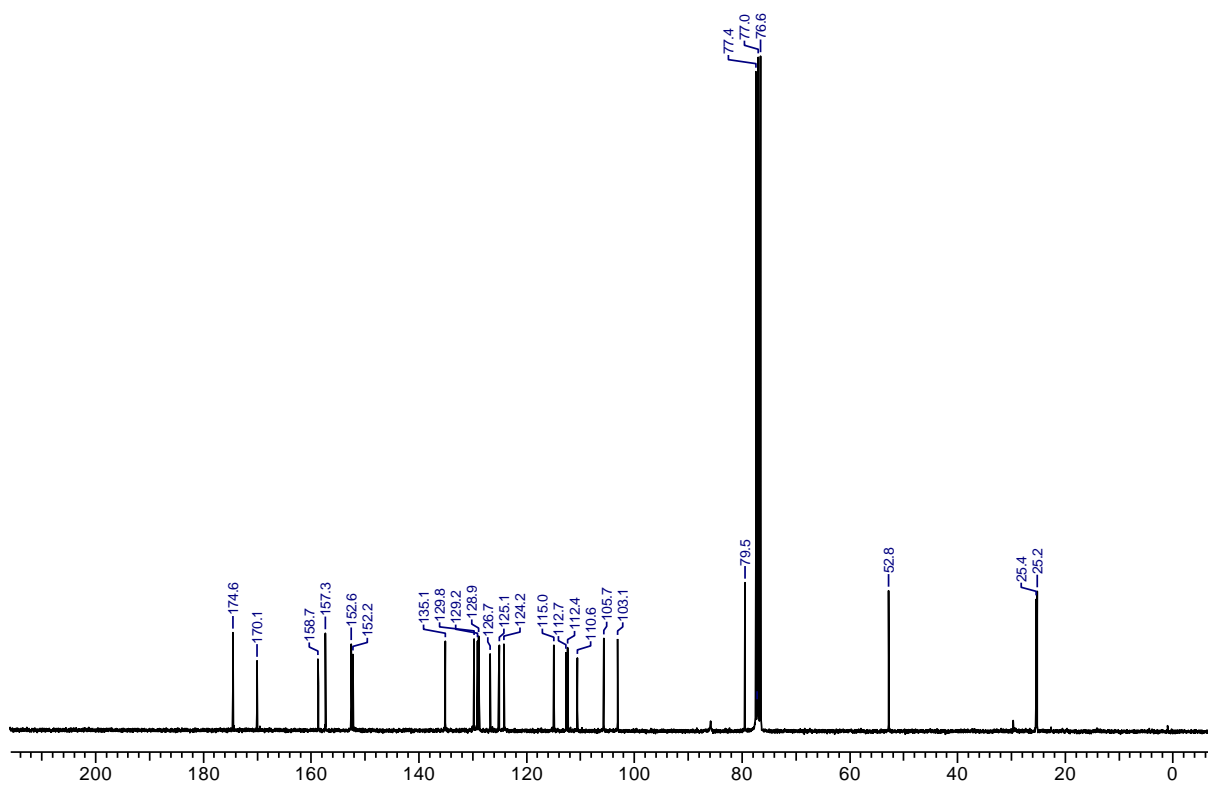


Figure S2. ^{13}C NMR spectrum of compound **6**.

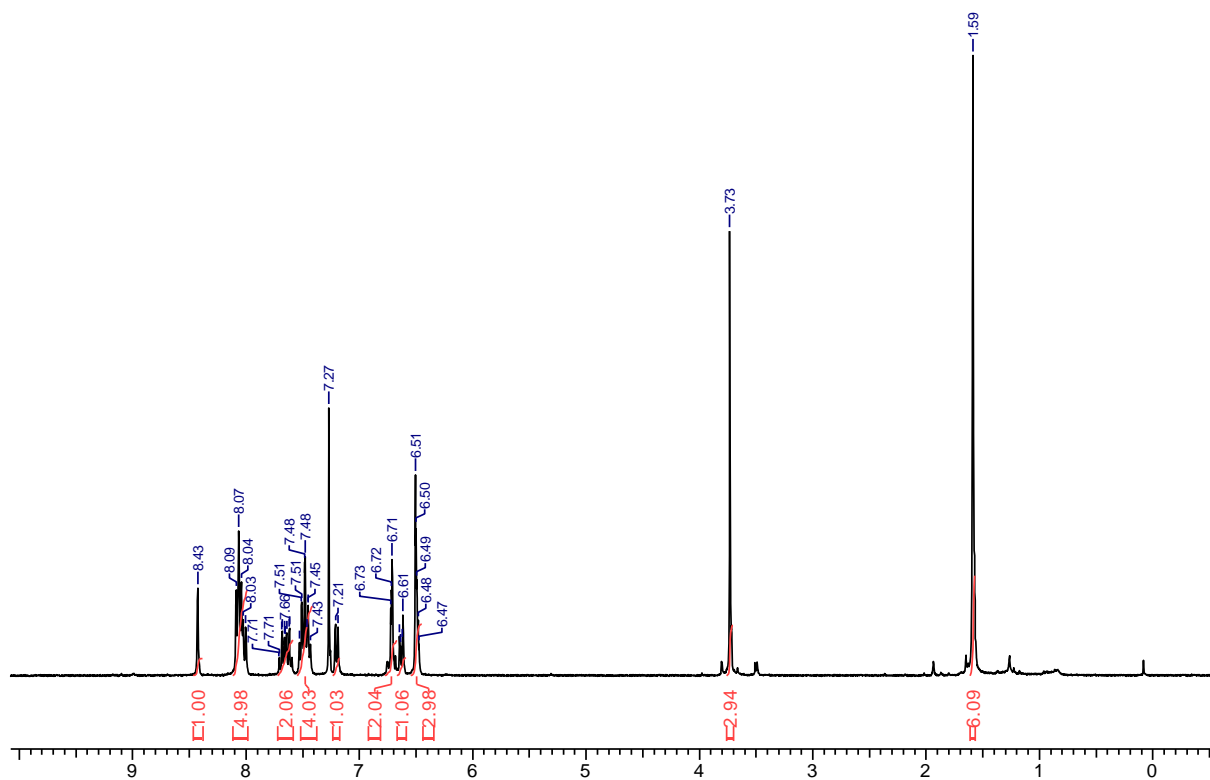


Figure S3. ^1H NMR spectrum of compound **7a**.

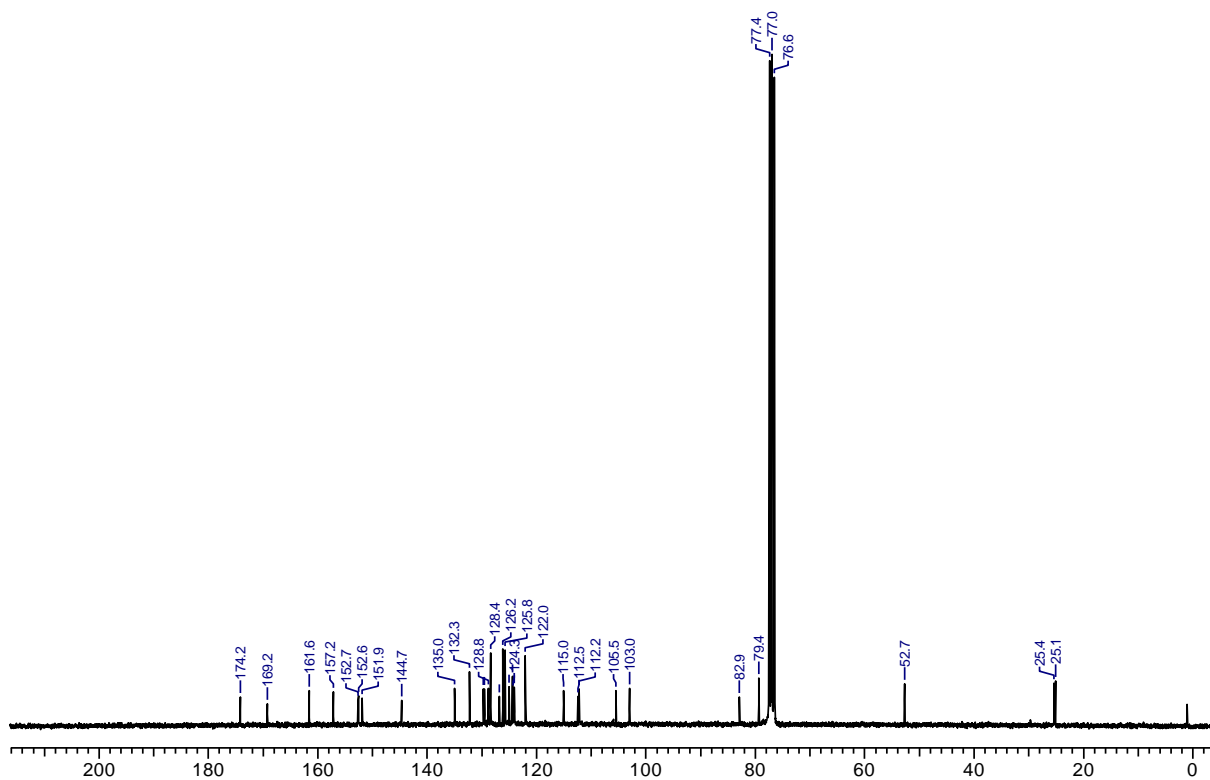


Figure S4. ^{13}C NMR spectrum of compound **7a**.

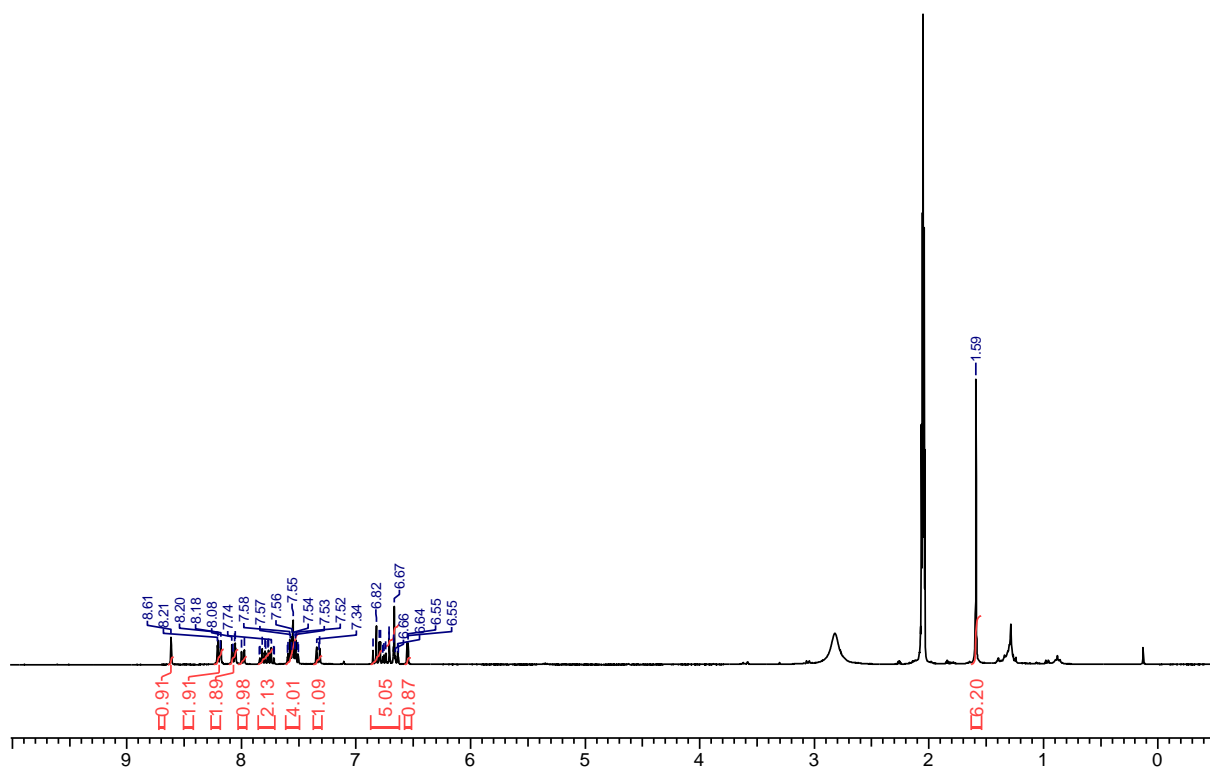


Figure S5. ^1H NMR spectrum of probe 4.

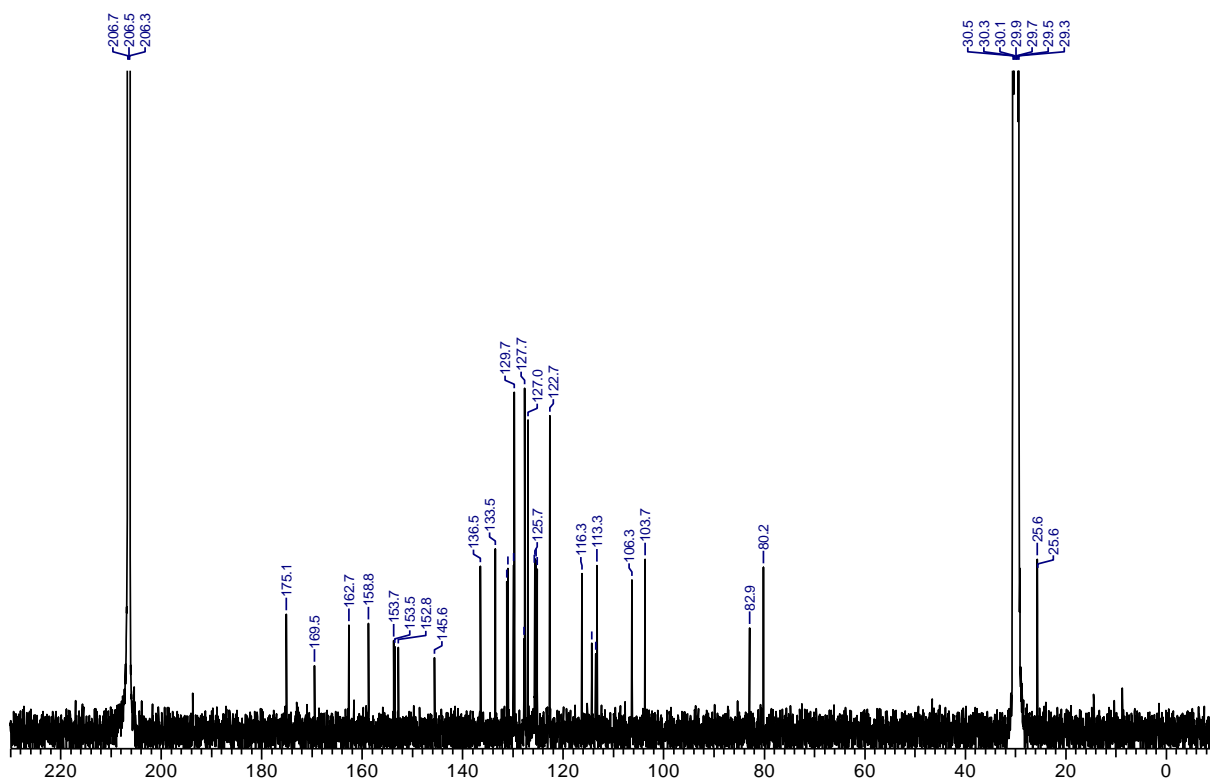


Figure S6. ^{13}C NMR spectrum of probe 4.

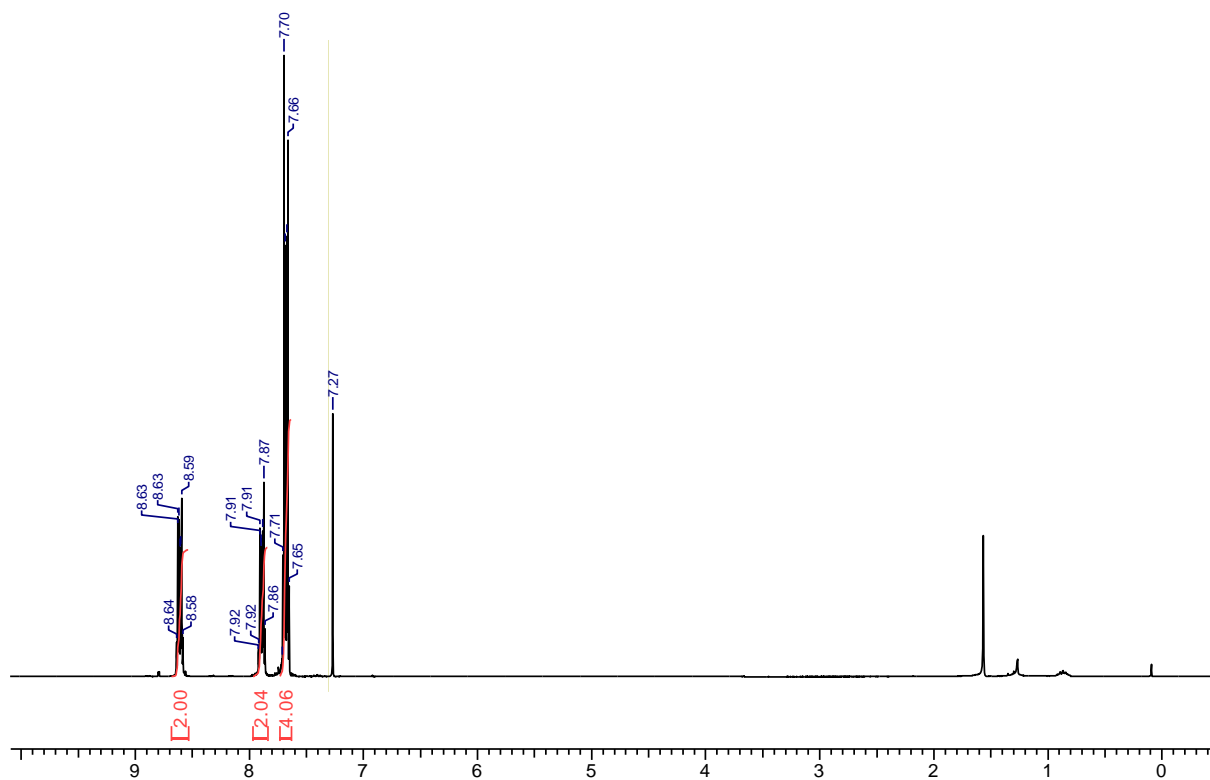


Figure S7. ^1H NMR spectrum of 9-bromo-10-nitroanthracene.

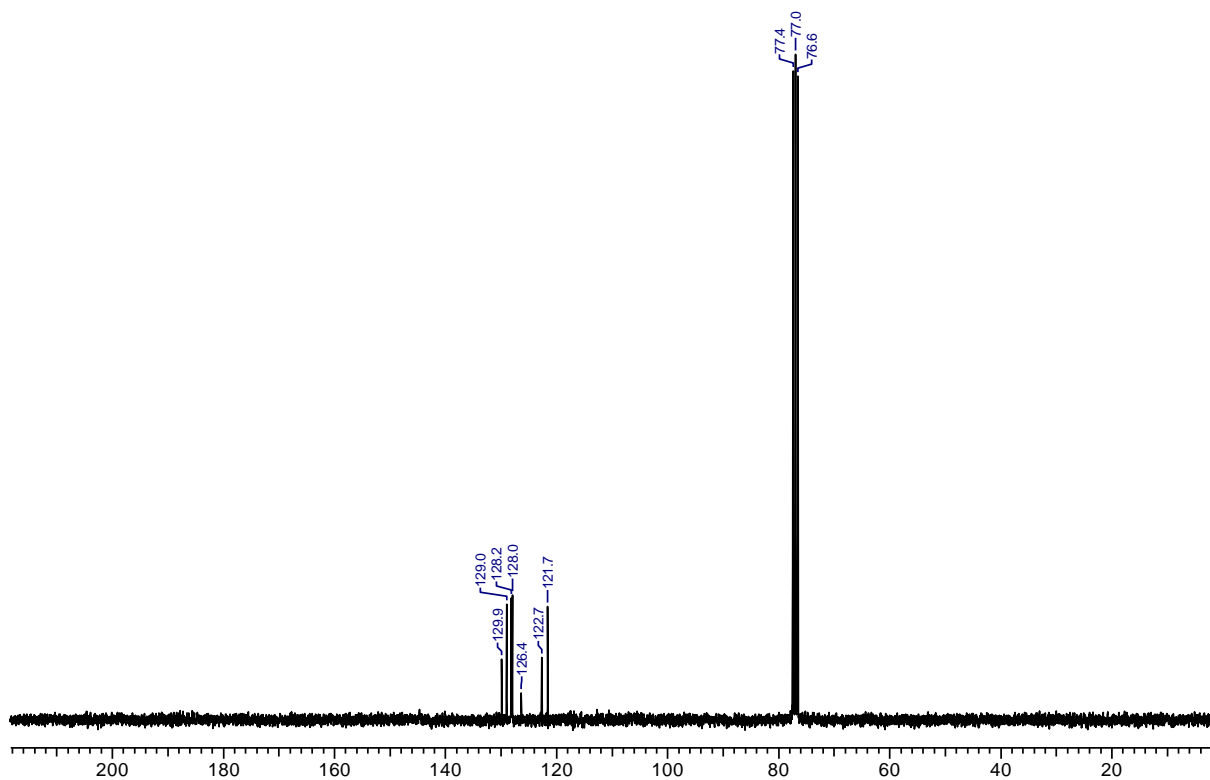


Figure S8. ^{13}C NMR spectrum of 9-bromo-10-nitroanthracene.

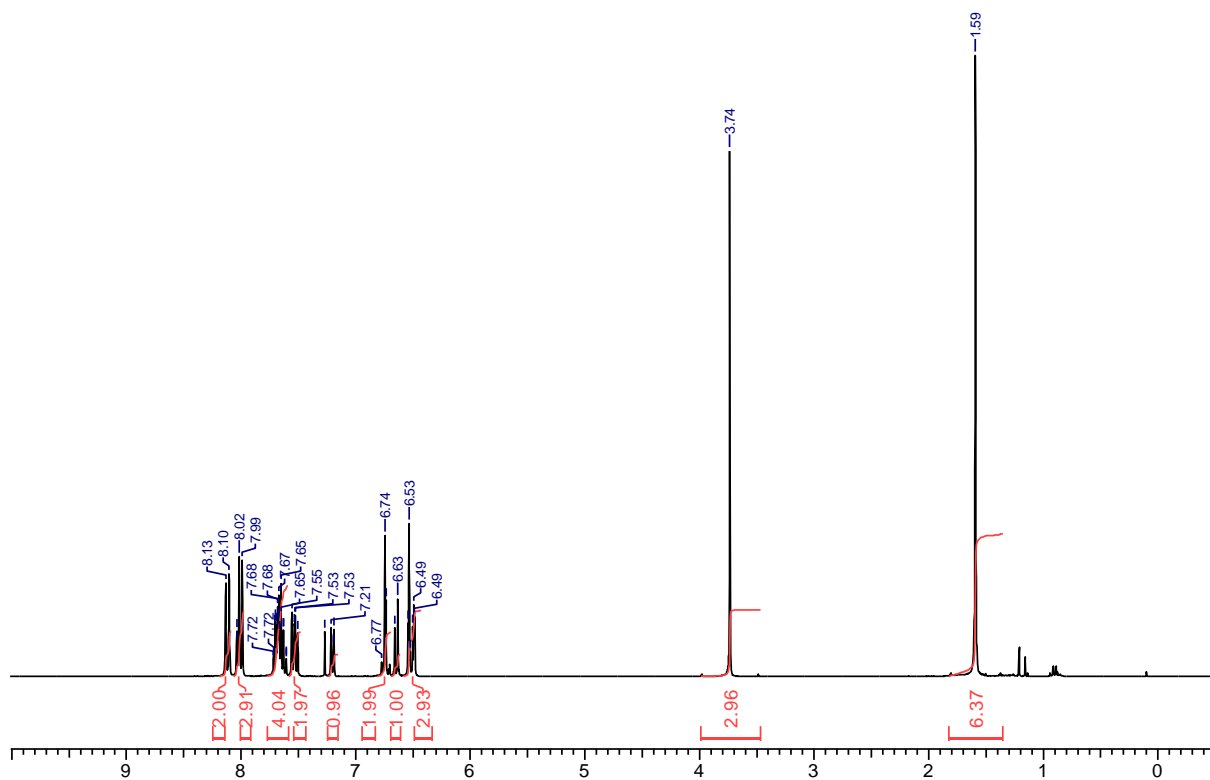


Figure S9. ^1H NMR spectrum of compound **7b**.

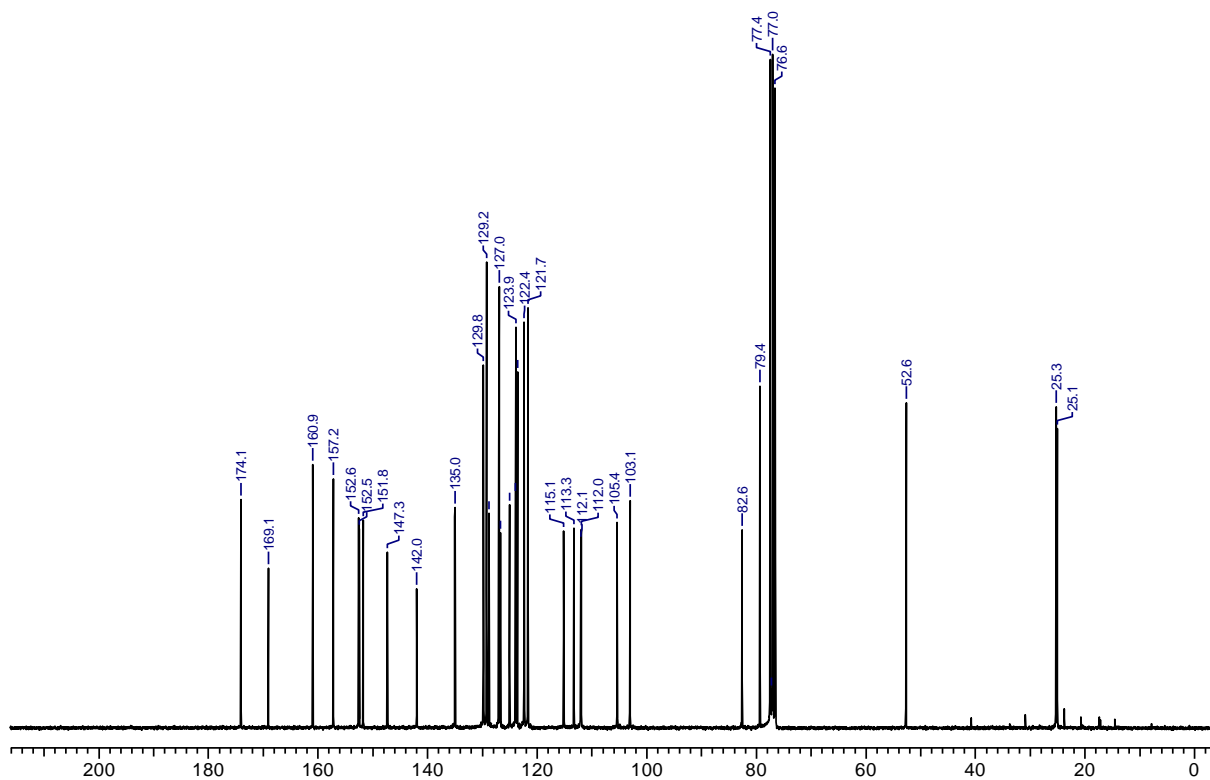


Figure S10. ^{13}C NMR spectrum of compound **7b**.

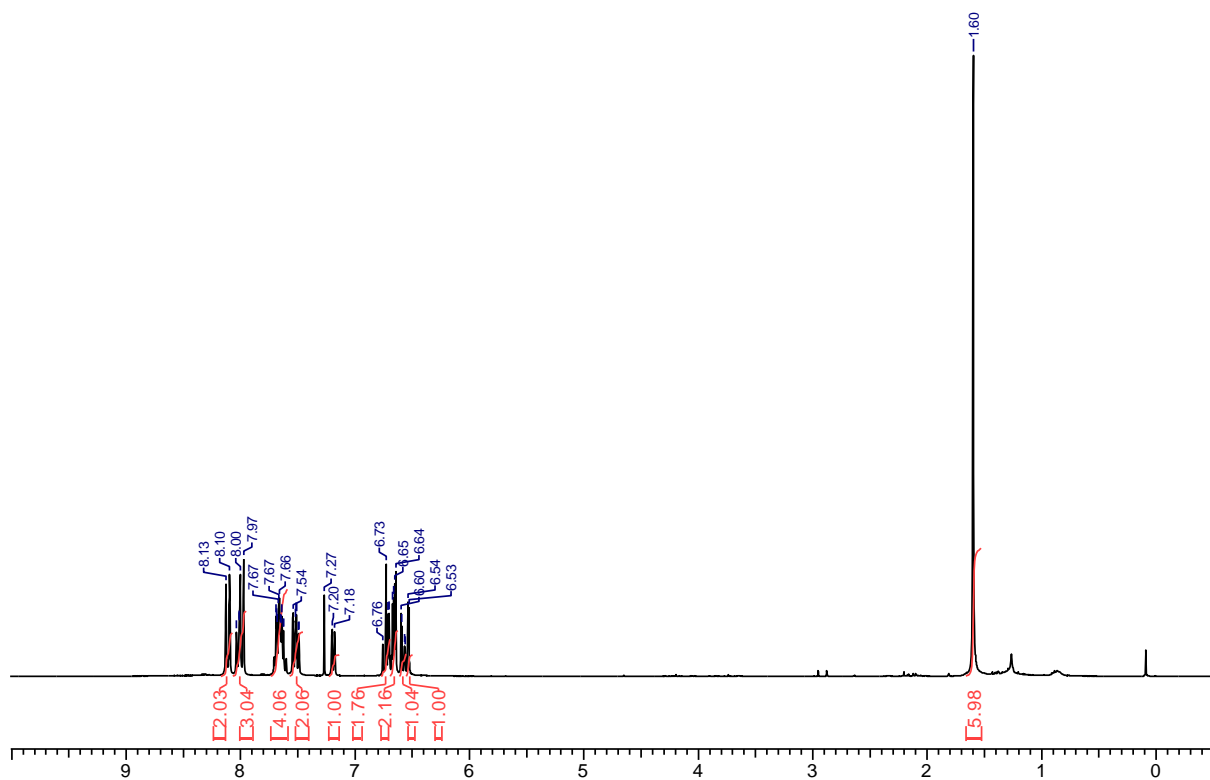


Figure S11. ^1H NMR spectrum of compound **8b**.

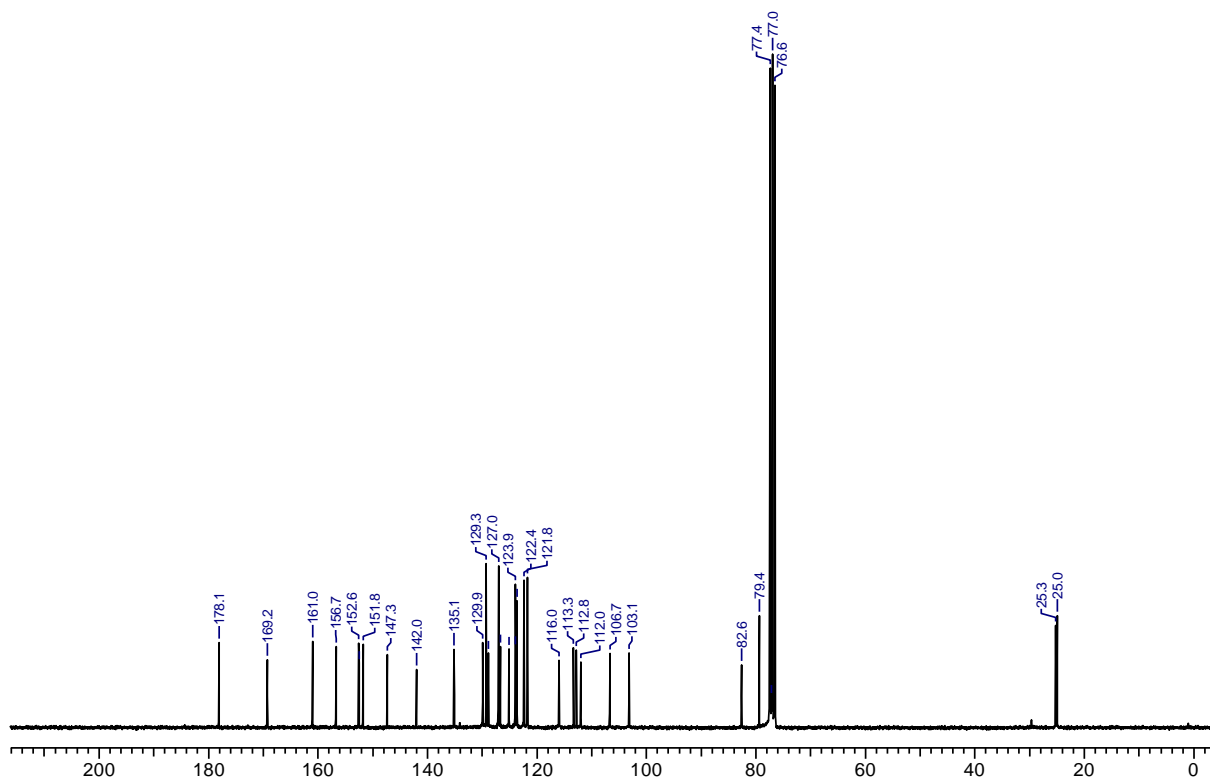


Figure S12. ^{13}C NMR spectrum of compound **8b**.

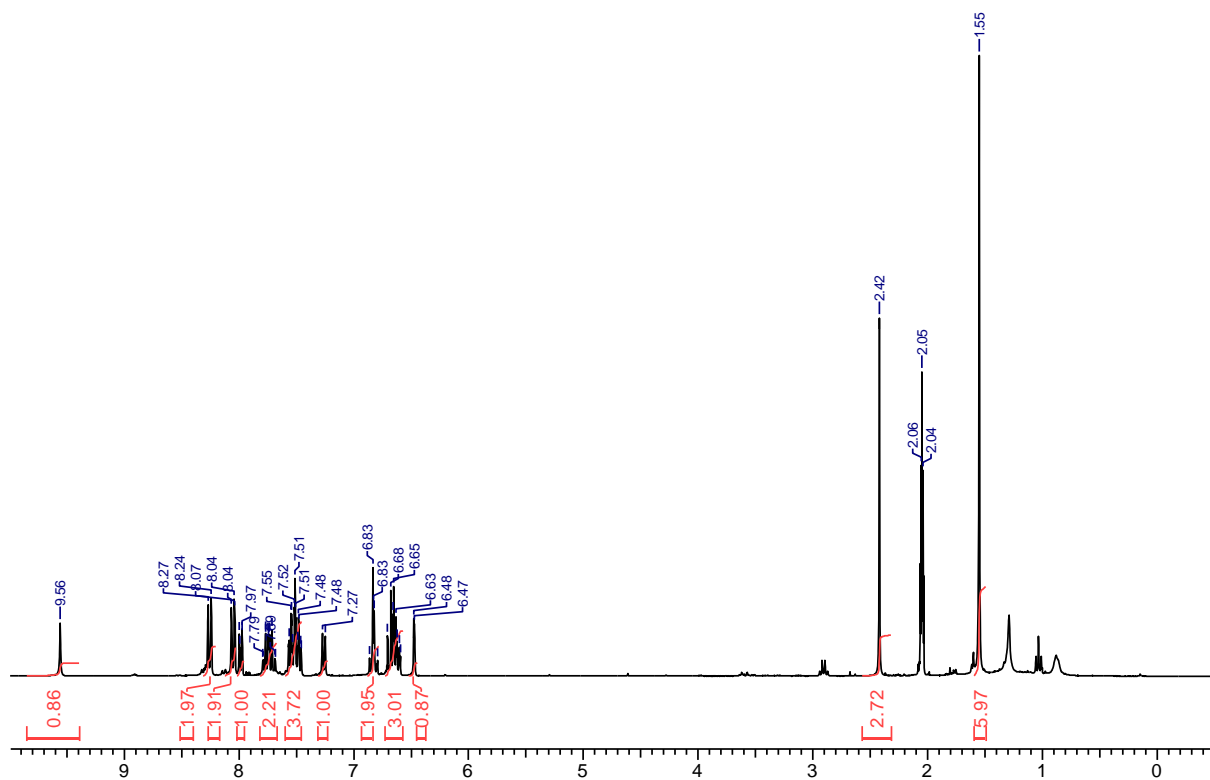


Figure S13. ^1H NMR spectrum of compound **8c**.

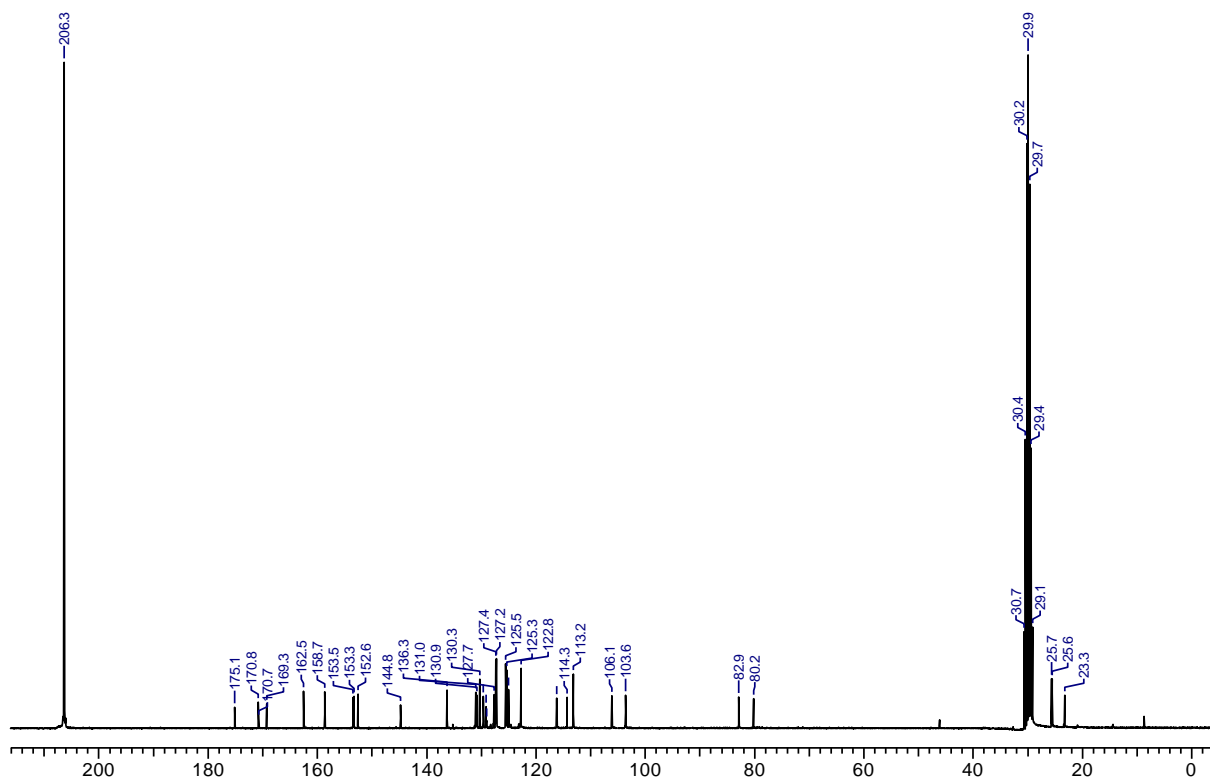


Figure S14. ^{13}C NMR spectrum of compound **8c**.

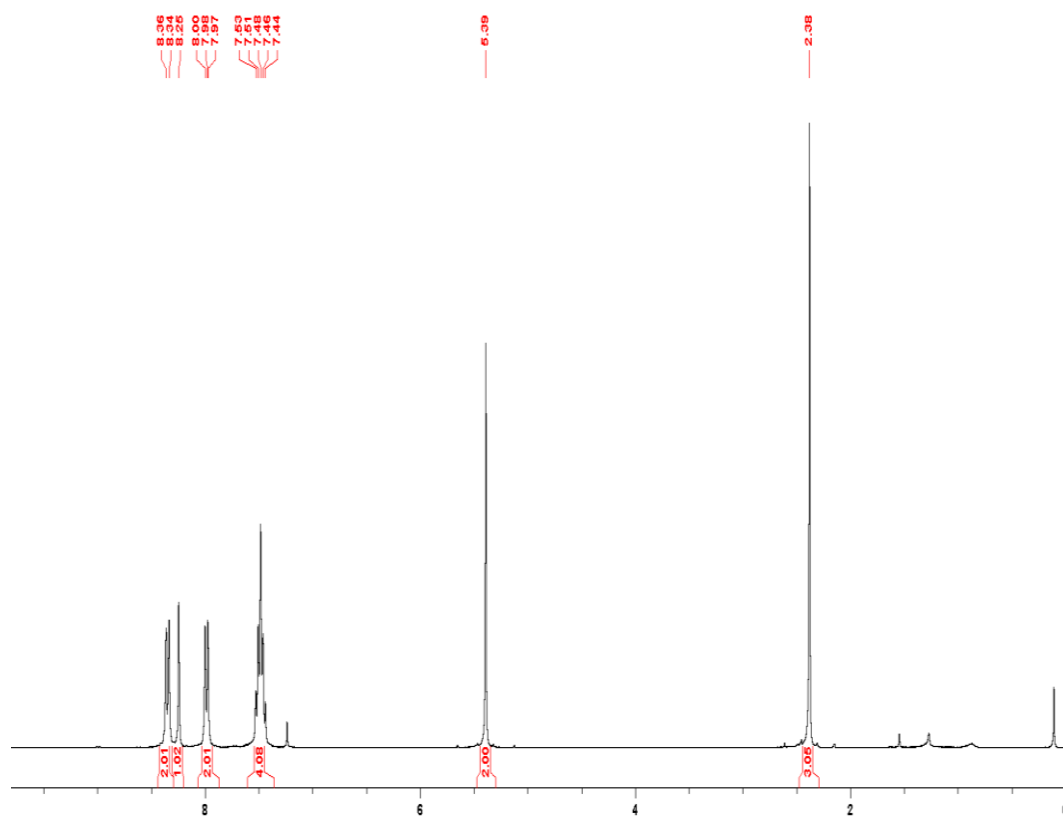


Figure S15. ^1H NMR spectrum of 9-(methylthiomethoxy)anthracene.

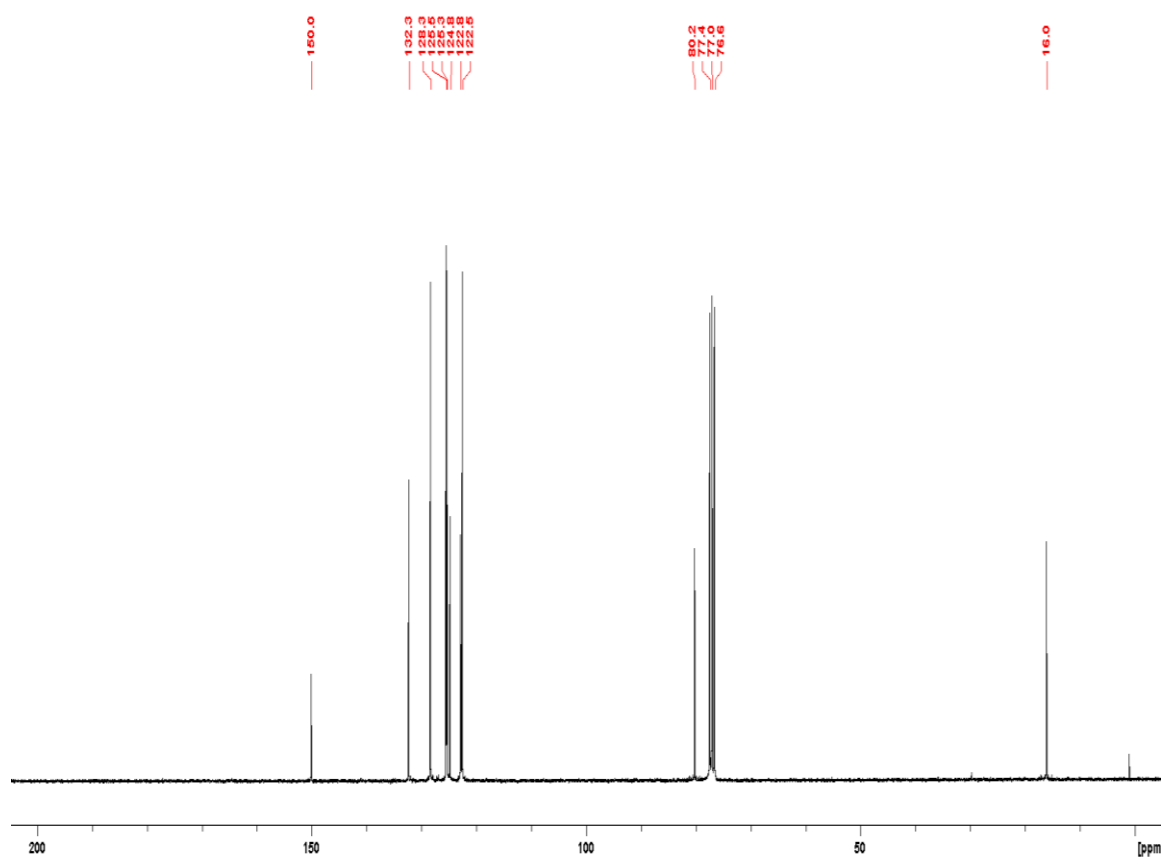


Figure S16. ^{13}C NMR spectrum of 9-(methylthiomethoxy)anthracene.

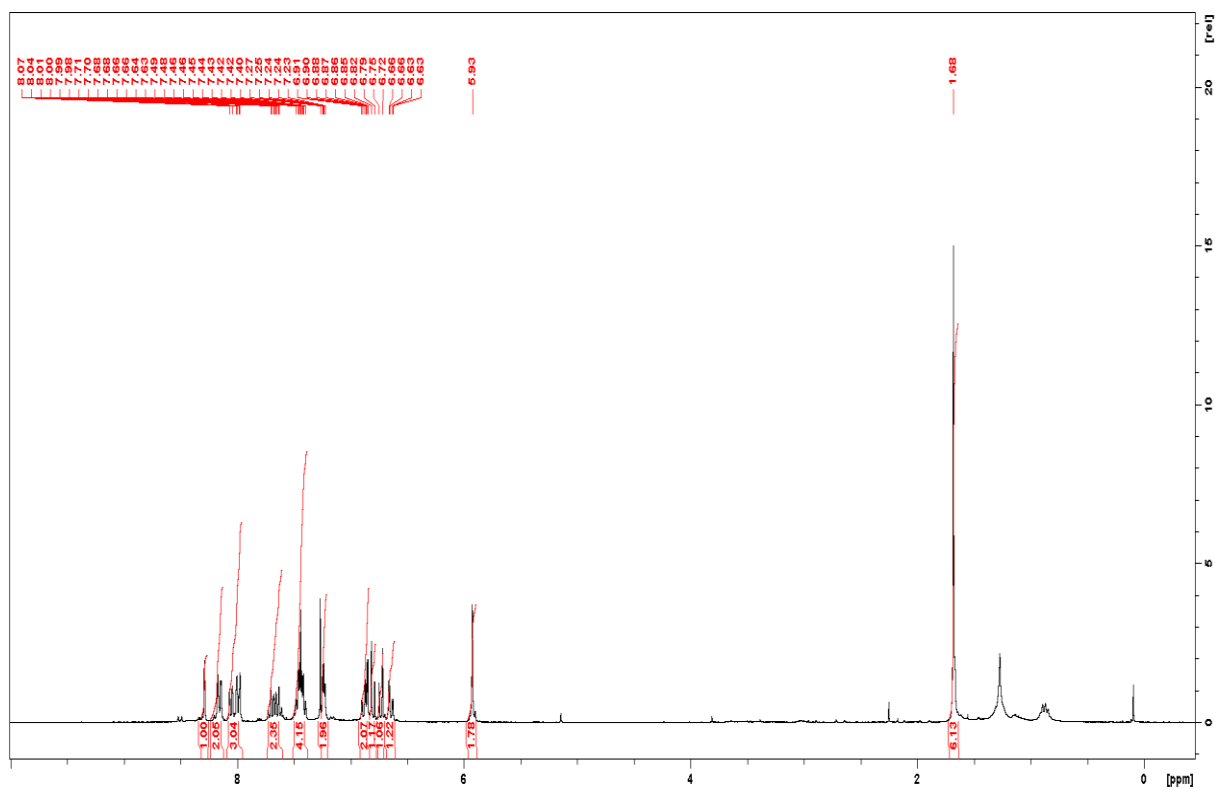


Figure S17. ¹H NMR spectrum of compound **8d**.

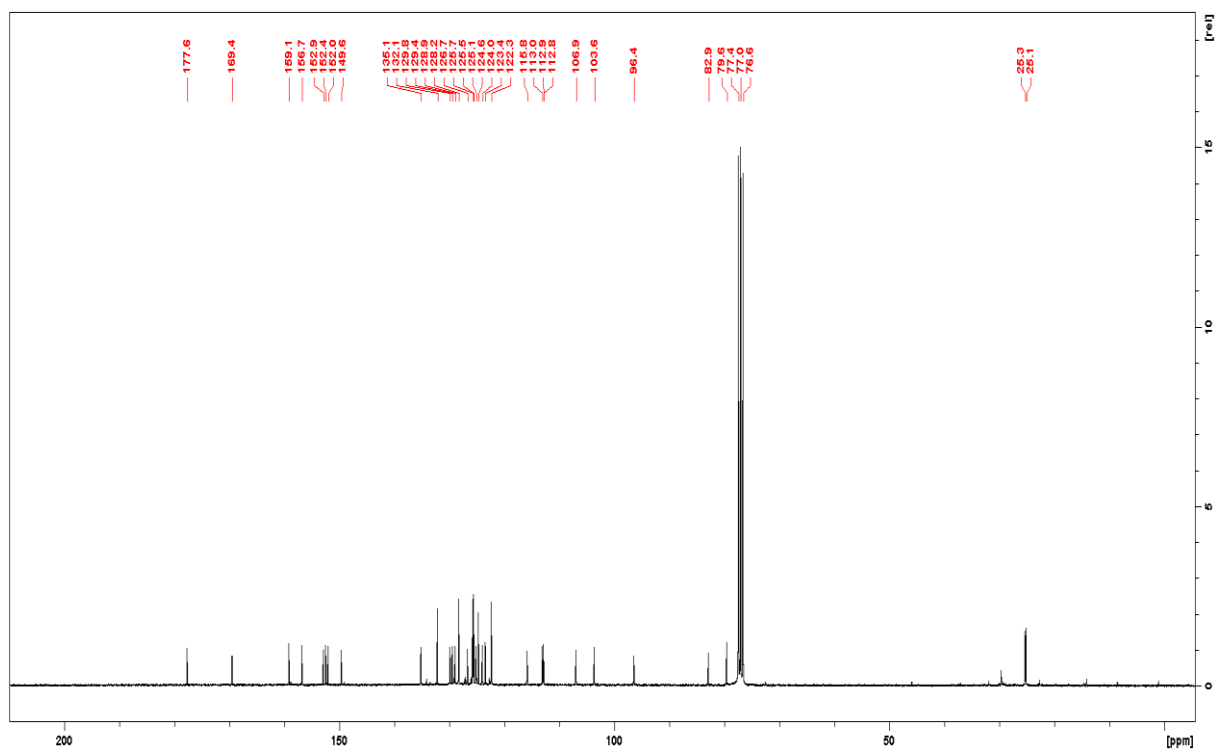


Figure S18. ¹³C NMR spectrum of compound **8d**.

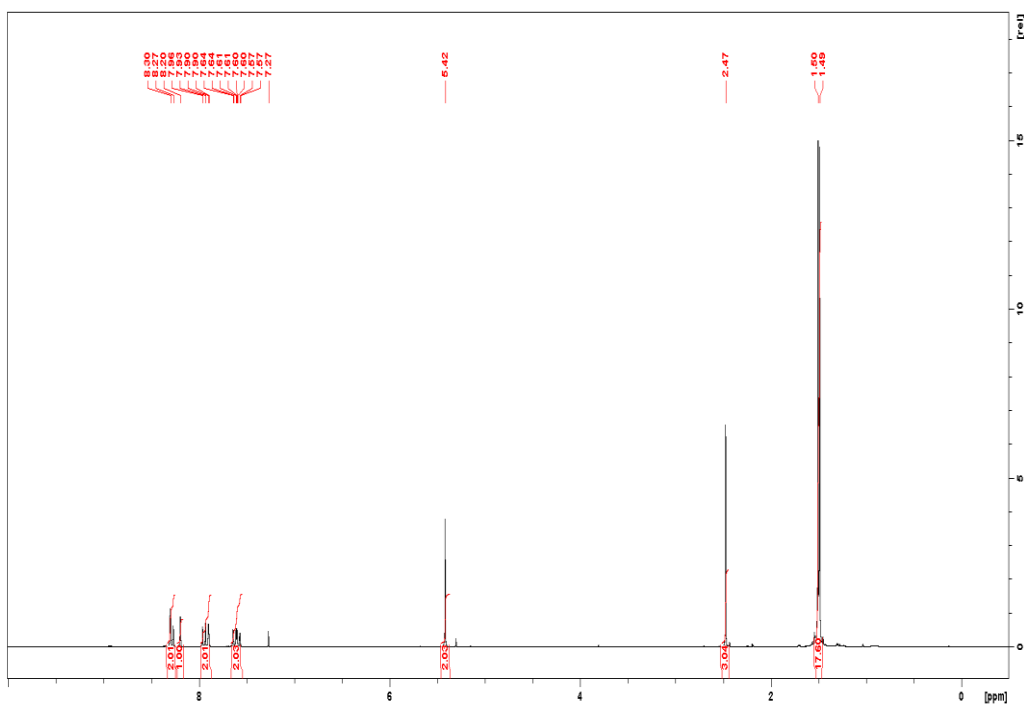


Figure S19. ^1H NMR spectrum of 2,6-di-*tert*-butyl-9-(methylthiomethoxy)anthracene.

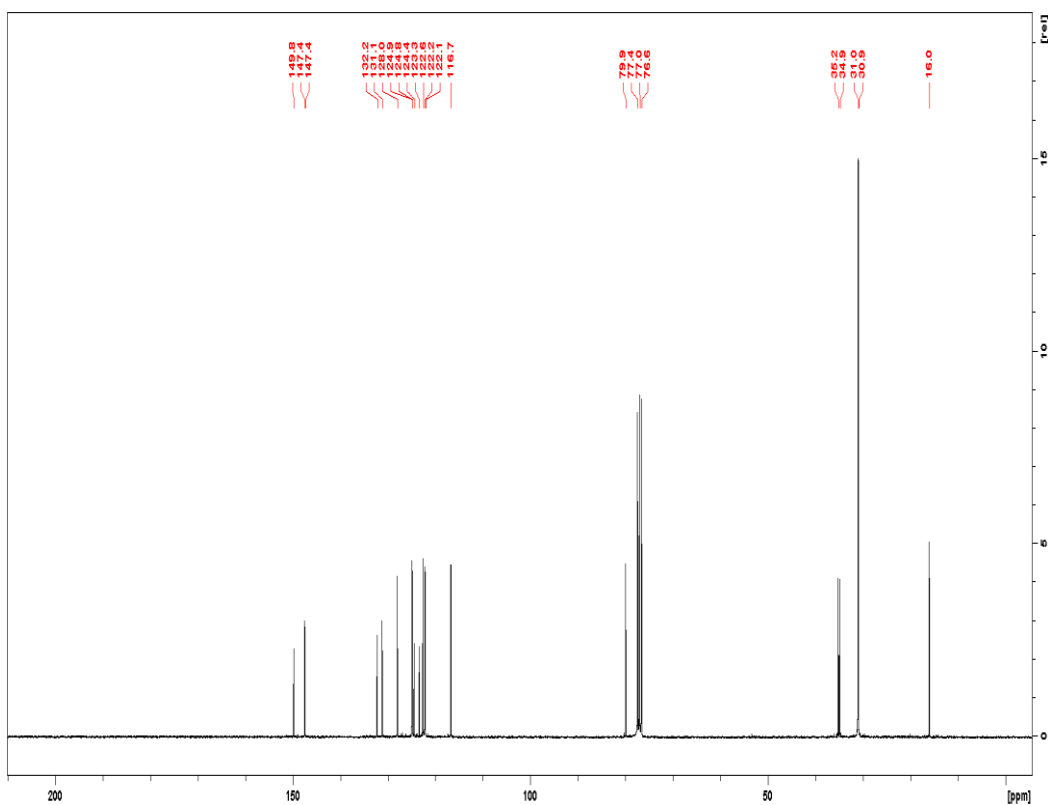


Figure S20. ^{13}C NMR spectrum of 2,6-di-*tert*-butyl-9-(methylthiomethoxy)anthracene.

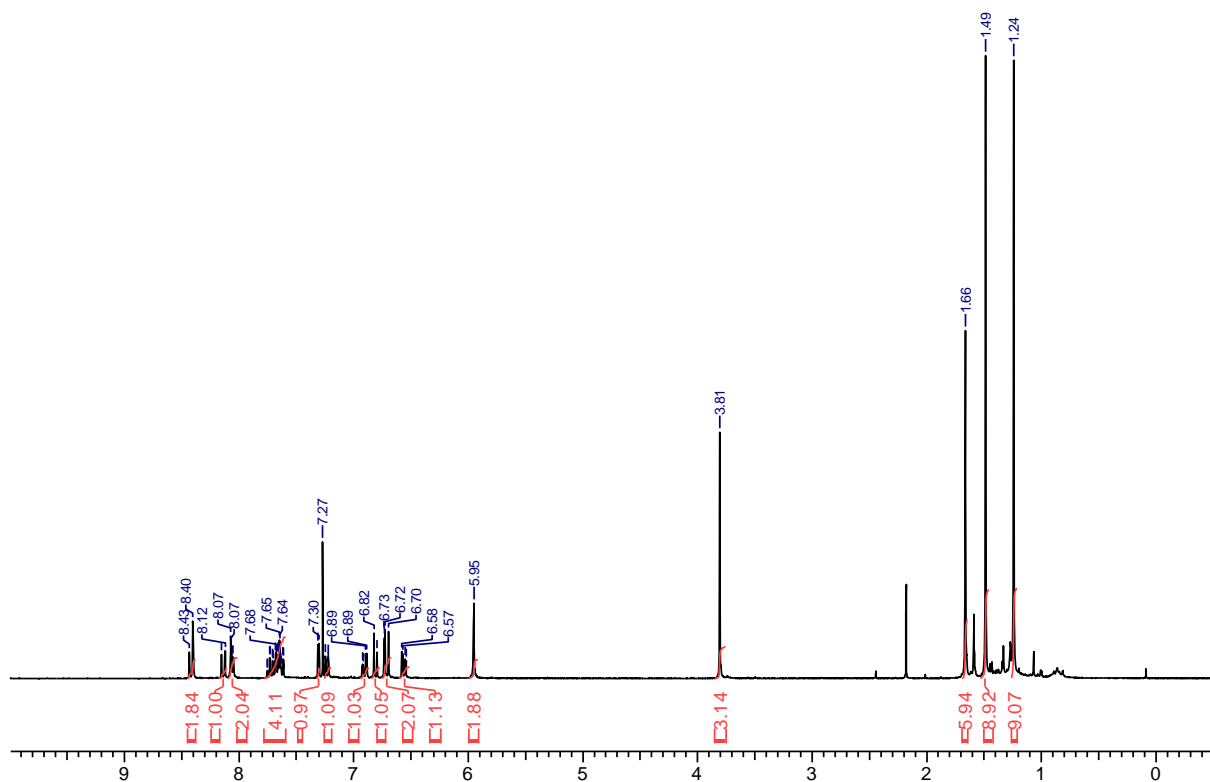


Figure S21. ^1H NMR spectrum of compound **7e**.

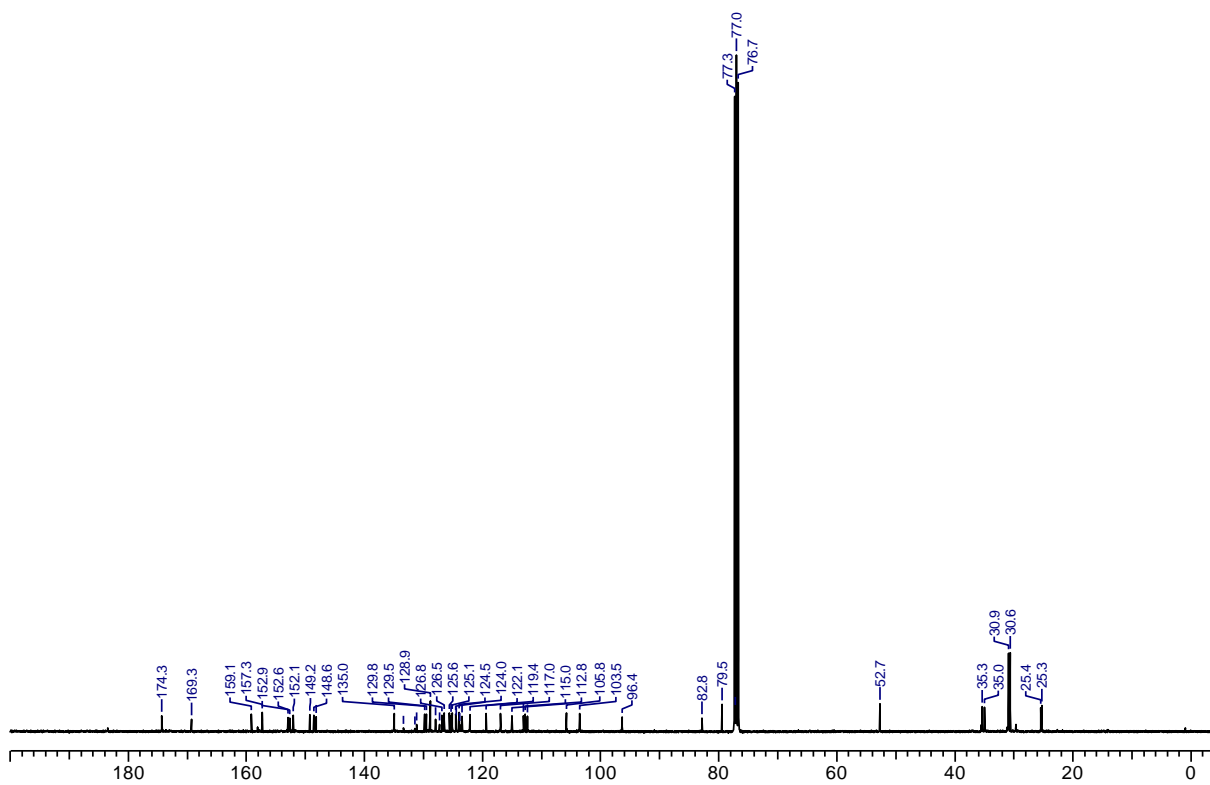


Figure S22. ^{13}C NMR spectrum of compound **7e**.

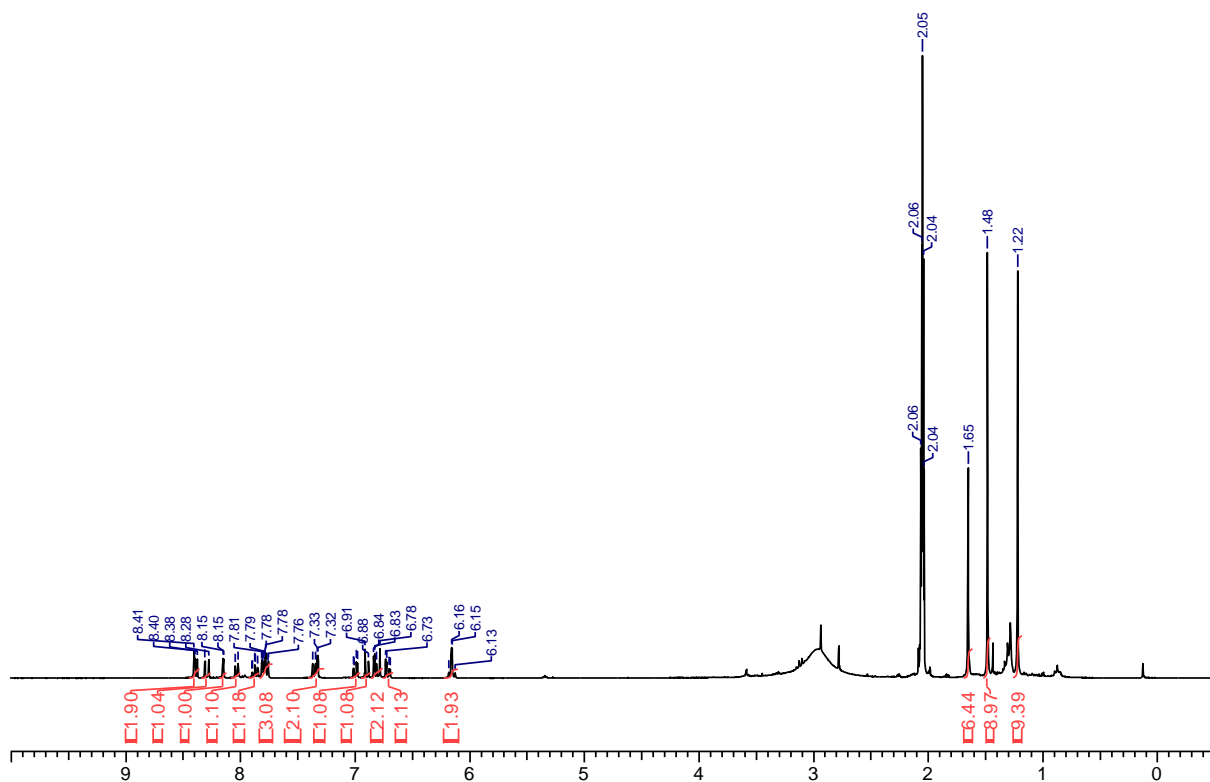


Figure S23. ^1H NMR spectrum of probe **8e**.

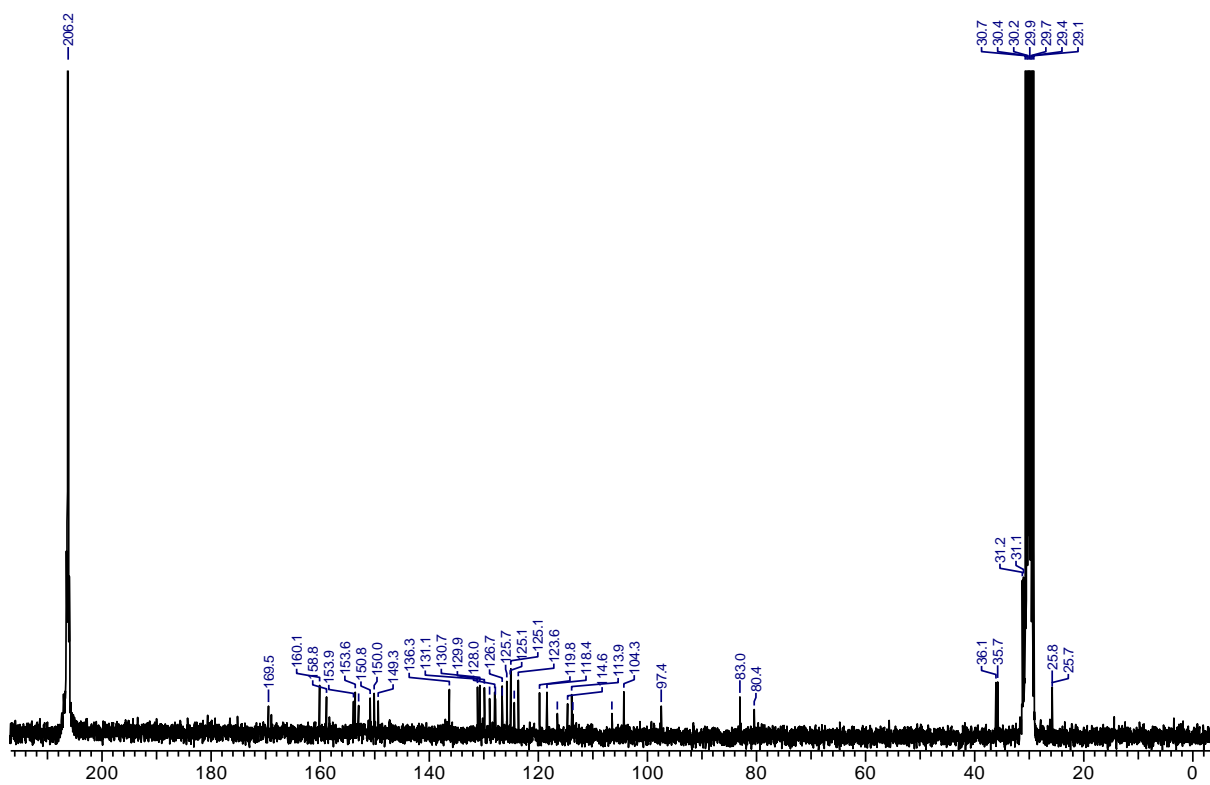
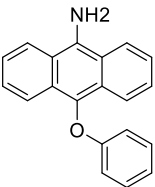
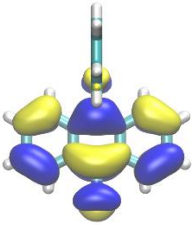
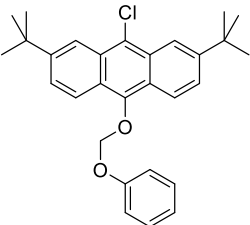
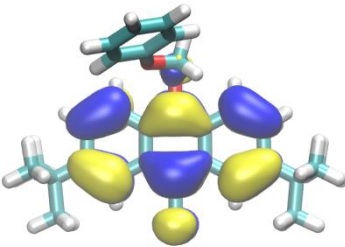
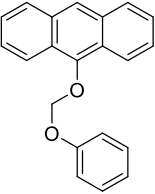
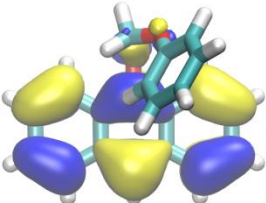


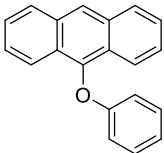
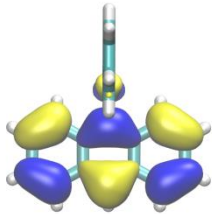
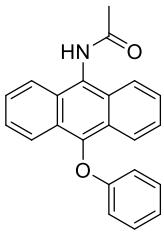
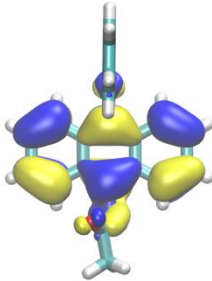
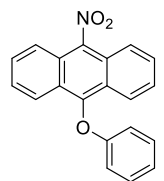
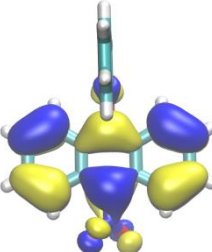
Figure S24. ^{13}C NMR spectrum of probe **8e**.

Calculation of energies of highest occupied orbitals (HOMOs) of simple models mimicking probes **4**, **8a-e**

Geometry optimizations were performed using the B3LYP¹ hybrid density functional and the 6-31G**²⁻¹¹ basis set with Gaussian16.¹² Frequency calculations of the optimized structures were used to confirm stationary points (minima). Checkpoint files were converted to formatted checkpoint files using the formchk command and cube files containing MO data were obtained with the cubegen command from the Gaussian suite. Visualization of the HOMO isosurfaces was performed with vmd 1.9.3,^{13, 14} using orbital isovalues of -0.02 (yellow) and 0.02 (blue).

Table S1.

Gaussian 16 (B3LYP/6-31G**)				
Probe	Model structure	HOMO energy [eV]	HOMO	Relative HOMO-energies [eV]
Reference		-4.77		reference, E=0
8e		-5.20		-0.43
8d		-5.20		-0.43

4		-5.27		-0.50
8c		-5.28		-0.51
8b		-5.78		-1.01

Intensity of green color in the last column of this table indicates the reactivity of the corresponding anthracene derivative with $^1\text{O}_2$ as predicted based on energies of the HOMOs.

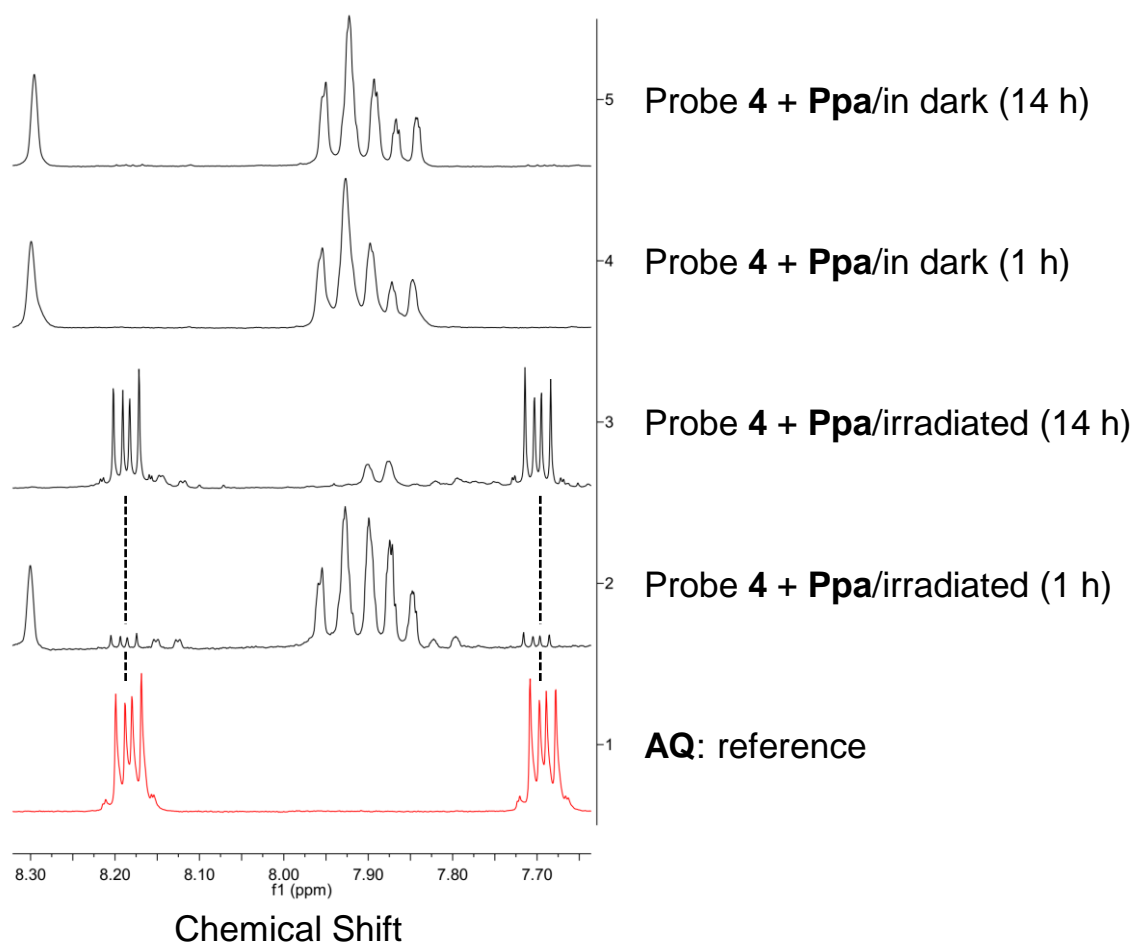


Figure **S25**. ¹H NMR spectroscopic monitoring conversion of probe **4** (5 mM) to anthraquinone **AQ** in the presence of photochemically generated ¹O₂. ¹O₂ was generated upon irradiation of photosensitizer pyropheophorbide a (Ppa, 0.1 eq, 0.5 mM) with red light (650 nm) for 1 h and 14 h. Spectrum of reference compound **AQ** is shown as a red trace. Peaks of **AQ** appearing upon the transformation of probe **4** are indicated with dotted, black lines.

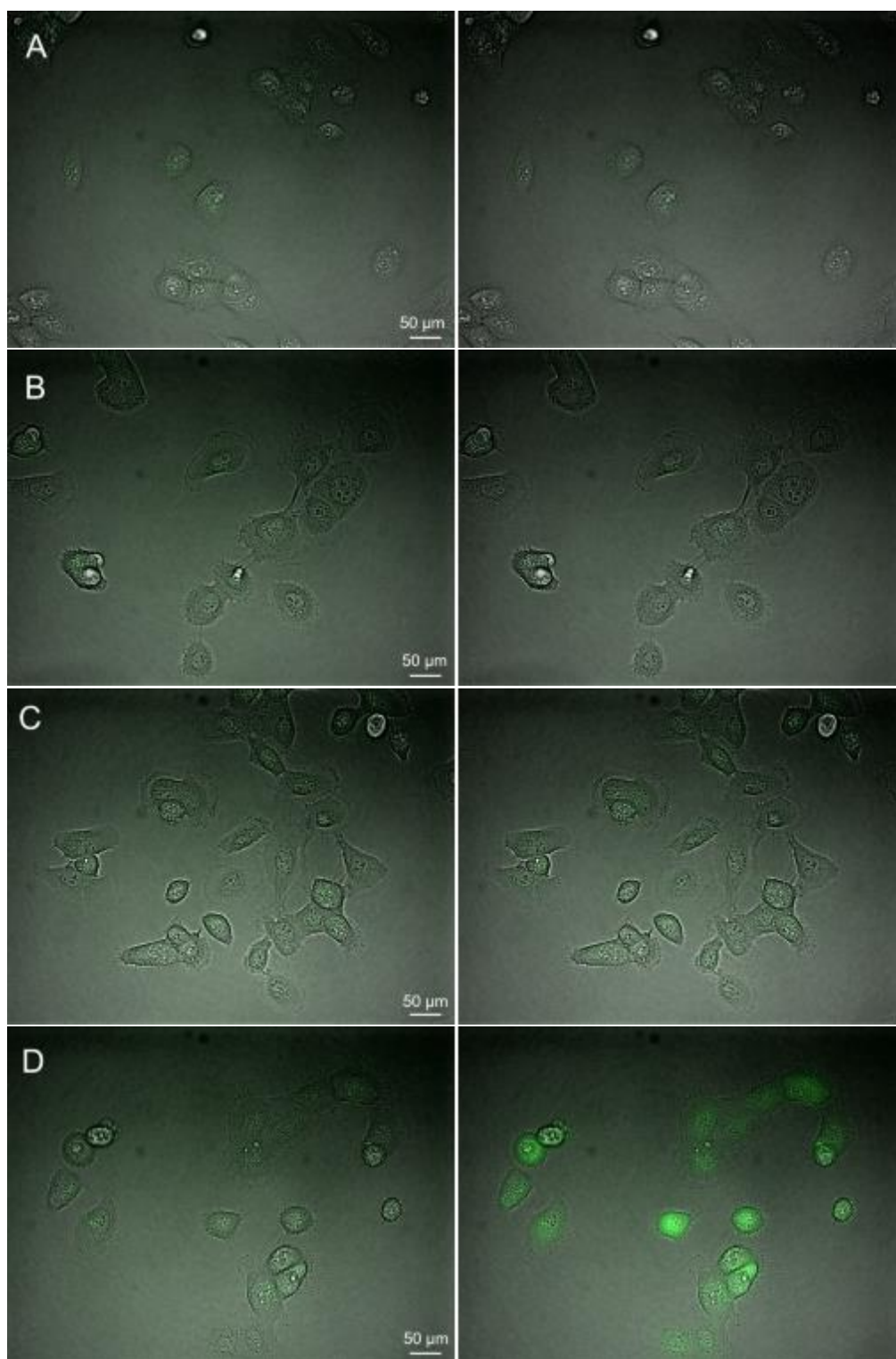


Figure **S26**. Fluorescence microscopy images combined with optical image of DU-145 cells before (left column) and after (right column) irradiation under red channel. A: Cells treated with a carrier DMF; B: Cells treated with probe **4** (1 μM); C: Cells treated with InPpa (0.1 μM); C: Cells treated with probe **4** (1 μM) and InPpa (0.1 μM).

References

1. A. D. Becke, *J. Chem. Phys.*, 1993, **98**, 5648-5652.
2. R. Ditchfield, W. J. Hehre and J. A. Pople, *J. Chem. Phys.*, 1971, **54**, 724-728.
3. W. J. Hehre, R. Ditchfield and J. A. Pople, *J. Chem. Phys.*, 1972, **56**, 2257-2261.
4. P. C. Hariharan and J. A. Pople, *Theor. Chem. Acc.*, 1973, **28**, 213-222.
5. P. C. Hariharan and J. A. Pople, *Mol. Phys.*, 1974, **27**, 209-214.
6. M. S. Gordon, *Chem. Phys. Lett.*, 1980, **76**, 163-168.
7. M. M. Francl, W. J. Pietro, W. J. Hehre, J. S. Binkley, D. J. DeFrees, J. A. Pople and M. S. Gordon, *J. Chem. Phys.*, 1982, **77**, 3654-3665.
8. R. C. Binning Jr. and L. A. Curtiss, *J. Comput. Chem.*, 1990, **11**, 1206-1216.
9. J.-P. Blaudeau, M. P. McGrath, L. A. Curtiss and L. Radom, *J. Chem. Phys.*, 1997, **107**, 5016-5021.
10. V. A. Rassolov, J. A. Pople, M. A. Ratner and T. L. Windus, *J. Chem. Phys.*, 1998, **109**, 1223-1229.
11. V. A. Rassolov, M. A. Ratner, J. A. Pople, P. C. Redfern and L. A. Curtiss, *J. Comput. Chem.*, 2001, **22**, 976-984.
12. M. J. Frisch, G. W. Trucks, H. B. Schlegel, G. E. Scuseria, M. A. Robb, J. R. Cheeseman, G. Scalmani, V. Barone, G. A. Petersson, H. Nakatsuji, X. Li, M. Caricato, A. V. Marenich, J. Bloino, B. G. Janesko, R. Gomperts, B. Mennucci, H. P. Hratchian, J. V. Ortiz, A. F. Izmaylov, J. L. Sonnenberg, Williams, F. Ding, F. Lipparini, F. Egidi, J. Goings, B. Peng, A. Petrone, T. Henderson, D. Ranasinghe, V. G. Zakrzewski, J. Gao, N. Rega, G. Zheng, W. Liang, M. Hada, M. Ehara, K. Toyota, R. Fukuda, J. Hasegawa, M. Ishida, T. Nakajima, Y. Honda, O. Kitao, H. Nakai, T. Vreven, K. Throssell, J. A. Montgomery Jr., J. E. Peralta, F. Ogliaro, M. J. Bearpark, J. J. Heyd, E. N. Brothers, K. N. Kudin, V. N. Staroverov, T. A. Keith, R. Kobayashi, J. Normand, K. Raghavachari, A. P. Rendell, J. C. Burant, S. S. Iyengar, J. Tomasi, M. Cossi, J. M. Millam, M. Klene, C. Adamo, R. Cammi, J. W. Ochterski, R. L. Martin, K. Morokuma, O. Farkas, J. B. Foresman and D. J. Fox, *Gaussian 16 Rev. B.01*, Wallingford, CT, 2016.
13. VMD web page, <http://www.ks.uiuc.edu/Research/vmd/>.
14. W. Humphrey, A. Dalke and K. Schulten, *J. Molec. Graphics*, 1996, **14**, 33-38.